

Regioselective Ultrafast Photoinduced Electron Transfer from Naphthols to Halocarbon Solvents

Subhajyoti Chaudhuri, Atanu Acharya, Erik T. J. Nibbering, and Victor S. Batista

J. Phys. Chem. Lett., Just Accepted Manuscript • DOI: 10.1021/acs.jpclett.9b00410 • Publication Date (Web): 03 May 2019

Downloaded from <http://pubs.acs.org> on May 4, 2019

Just Accepted

“Just Accepted” manuscripts have been peer-reviewed and accepted for publication. They are posted online prior to technical editing, formatting for publication and author proofing. The American Chemical Society provides “Just Accepted” as a service to the research community to expedite the dissemination of scientific material as soon as possible after acceptance. “Just Accepted” manuscripts appear in full in PDF format accompanied by an HTML abstract. “Just Accepted” manuscripts have been fully peer reviewed, but should not be considered the official version of record. They are citable by the Digital Object Identifier (DOI®). “Just Accepted” is an optional service offered to authors. Therefore, the “Just Accepted” Web site may not include all articles that will be published in the journal. After a manuscript is technically edited and formatted, it will be removed from the “Just Accepted” Web site and published as an ASAP article. Note that technical editing may introduce minor changes to the manuscript text and/or graphics which could affect content, and all legal disclaimers and ethical guidelines that apply to the journal pertain. ACS cannot be held responsible for errors or consequences arising from the use of information contained in these “Just Accepted” manuscripts.



ACS Publications

is published by the American Chemical Society, 1155 Sixteenth Street N.W., Washington, DC 20036

Published by American Chemical Society. Copyright © American Chemical Society. However, no copyright claim is made to original U.S. Government works, or works produced by employees of any Commonwealth realm Crown government in the course of their duties.

1
2
3
4 **Regioselective Ultrafast Photoinduced Electron**
5
6
7
8 **Transfer from Naphthols to Halocarbon Solvents**
9

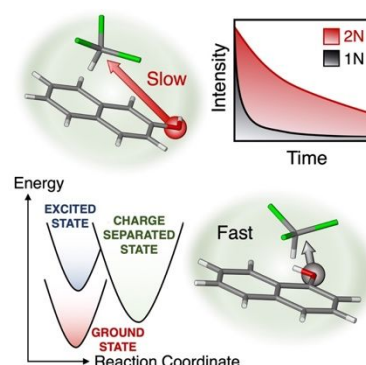
10
11
12 *Subhajyoti Chaudhuri[†], Atanu Acharya[†], Erik T J Nibbering[‡], and Victor S Batista^{†,*}*
13
14

15
16 [†] Department of Chemistry, P.O. Box 208107, Yale University, New Haven, CT 06520, USA
17
18

19 [‡] Max Born Institut für Nichtlineare Optik and Kurzzeitspektroskopie, Max Born Strasse 2A,
20
21 12489 Berlin, Germany
22
23
24
25
26
27
28
29
30
31
32
33
34
35
36
37
38
39
40
41
42
43
44
45
46
47
48
49
50
51
52
53
54
55
56
57
58
59
60

ABSTRACT: Excited state decay of 2-naphthol (2N) in halocarbon solvents has been observed to be significantly slower when compared to 1-naphthol (1N). In this study, we provide new physical insights behind this observation by exploring the regioselective electron transfer (ET) mechanism from photoexcited 1N and 2N to halocarbon solvents at a detailed molecular level. Using state-of-the-art electronic-structure calculations, we explore several configurations of naphthol-chloroform complexes, and find that the proximity of the electron accepting chloroform molecule to the electron-rich –OH group of the naphthol is the dominant factor affecting electron transfer rates. The origin of significantly slower electron transfer rates for 2N is traced back to the notably smaller electronic coupling when the electron accepting chloroform molecule is on top of the aromatic ring distal to the –OH group. Our findings suggest that regioselective photoinduced electron transfer could thus be exploited to control electron transfer in substituted acenes tailored for specific applications.

TOC GRAPHIC



1
2
3 Photoinduced electron transfer plays a key role in light harvesting molecular systems responsible
4 for converting electromagnetic radiation into charge carriers.^{1–6} Excited state processes are limited
5 by the excited state lifetimes. The radiative decay pathway competes with the non-radiative
6 pathways and typically involves charge separation and/or chemical changes. Understanding the
7 molecular mechanisms of excited state decay is thus essential for a wide range of applications.
8
9 One of the most important decay processes is via intermolecular electron transfer (ET), which is
10 the focus of this paper.
11
12

13
14 Significant efforts have been undertaken to elucidate ET processes by tuning the donor-acceptor
15 interactions through variation of molecular structures,⁷ or by control of ET rates through molecular
16 design of donor-acceptor dyad systems.^{8–10} Time-resolved spectroscopic studies have revealed the
17 relevant ET time-scales as well as geometric aspects that control the relaxation mechanisms by
18 regulating the arrangement and separation of specific donor and acceptor units.¹¹ The interplay
19 between fast “on-contact” ET reaction dynamics, and slow diffusional dynamics often makes it
20 difficult to interpret solution-phase ET between freely moving donor and acceptor systems, and
21 further intricacies occur upon the involvement of excited radical ion states.¹² Molecular design of
22 donor-acceptor dyads with fixed donor-acceptor distances has enabled the analysis of electron
23 transfer rates, as a function of free energy changes for a series of electron-acceptor moieties,
24 eliminating the ambiguity that would otherwise be introduced with variable electron donor-
25 acceptor distances.^{13–15} However, photoinduced electron transfer from solute to solvent is more
26 difficult to characterize because of the bulk nature of the solvent.^{16,17} Many solute-solvent
27 conformations are conducive to faster ET, whereas other configurations would be ineffective.
28 Nevertheless, conformations leading to fast ET often make photoinduced electron transfer the most
29 effective decay pathway. In fact, ET is often dominated by close contact interactions with the
30
31
32
33
34
35
36
37
38
39
40
41
42
43
44
45
46
47
48
49
50
51
52
53
54
55
56
57
58
59
60

1
2
3 fluctuating first coordination shell of solvent generating a distribution of solute-solvent
4 configurations without significant diffusional character of donor-acceptor partners. This aspect has
5 been understood to play a crucial role in donor-acceptor systems where the aromatic nature of both
6 donor and acceptor makes the $\pi - \pi$ orbital interactions the dominating factor. Examples for
7 these can be found in important time-resolved ET studies using N,N-dimethylaniline as electron
8 donating solvent and a variety of aromatic electron acceptors.¹⁸⁻²³ The size of such molecular
9 systems makes computations prohibitively expensive with state-of-the-art quantum chemical
10 calculational methodology. Hence, we first study a significantly more compact halocarbon solvent
11 as an electron accepting case, with a moderately sized naphthol as the electron donor. With this,
12 we analyze thermally accessible configurations to identify dominant configurations for efficient
13 ET.
14
15

16 Previous studies have ascribed ET from electronically excited naphthol to the non-polar carbon
17 tetrachloride (CCl_4) solvent as the main mechanism for ultrafast fluorescence decay, as observed
18 by Time-Correlated Single Photon Counting (TCSPC) experiments.^{24,25} However, a mechanism
19 that could explain the appreciably slower excited state decay of 2-naphthol (2N) compared to 1-
20 naphthol (1N) remains unknown and is the subject of this paper.
21
22

23 Here, we find new physical evidence for the photoinduced electron transfer mediated decay of the
24 naphthol excited state making the photoinduced electron transfer from 1N much faster than from
25 2N. We focus on studying ET to the solvent by explicitly modeling the electron accepting solvent
26 in complexation with the solute. We explore a distribution of configurations for the naphthol
27 chromophore in close contact with the electron acceptor solvent in the first coordination sphere,
28 while modeling the rest of the surrounding solvent as a polarizable continuum dielectric.
29
30
31
32
33
34
35
36
37
38
39
40
41
42
43
44
45
46
47
48
49
50
51
52
53
54
55
56
57
58
59
60

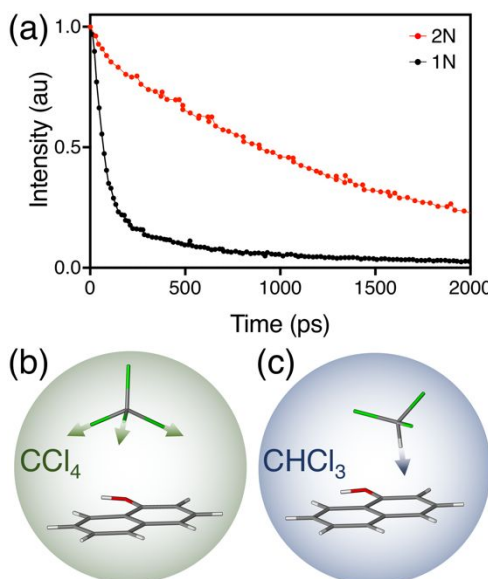


Figure 1. (a) TCSPC measurements of 1N and 2N in CHCl_3 . (b) Optimized ground state geometry of 1N in CCl_4 showing C-Cl bonds forming an umbrella-like configuration on the naphthol. (c) CHCl_3 with the C-H bond pointing towards the naphthol aromatic ring.

We focus on chloroform since it is a solvent probe with directional character that allows for a systematic exploration of interactions in the electron donor-acceptor complex. Polar solvents like water were ruled out since they would lead to chemical changes resulting from the photoacidic property of naphthols, thus defeating the purpose of studying photoinduced electron transfer. A previous ET-mediated fluorescence quenching study was focused on CCl_4 , a solvent without significant directionality.²⁴ The CCl_4 molecule interacts with the aromatic ring of naphthols, with the three C-Cl bonds forming an umbrella-like arrangement facing the naphthol fluorophore (Figure 1(b)).

Remarkably, the electronic excited state decay times differ by an order of magnitude when comparing 1N and 2N (1.4 ps in 1N vs. 13 ps in 2N, as measured by UV/IR pump-probe spectroscopy) in CCl_4 . The difference is even more significant in chloroform (70 ps in 1N vs. 900

ps-1.9 ns in 2N), with 2N again exhibiting the slower decay (Figure 1(a)). Chloroform (CHCl_3) in the first solvation shell has the C-H bond usually pointing towards the naphthol (Figure 1(c)) thus functioning as a directional probe.

The analysis of energetically accessible configurations of naphthol- CHCl_3 complexes reveals that proximity of the electron accepting solvent molecule to the proximal aromatic ring ($\text{R}^{(1)}$), as the primary factor governing the ET rates. The close contact arrangement provides understanding of configurations that dominate photoinduced electron transfer in naphthols, providing a design principle for modulation of ET with $-\text{OH}$ substituted polyacene electron donors.

The configurations of 1N and 2N in contact with CHCl_3 were obtained in a continuum dielectric environment, as described by the CPCM²⁶ model in Q-Chem 5.0.²⁷ The CHCl_3 electron acceptor was found to settle on top of the naphthol (Figure 2(d)) with the C-H bond pointing towards one of the rings ($\text{R}^{(1)}$ or $\text{R}^{(2)}$), as described by the ground electronic state at the B3LYP²⁸-D (empirical dispersion correction from Chai & Head-Gordon²⁹)/6-31+G(d,p) level of theory.

In non-polar or weakly polar solvents, the $^1\text{L}_a$ state is higher than the $^1\text{L}_b$ state. Thus, following Kasha's rule, only the $^1\text{L}_b$ state emission is observed since fluorescence emission is observed from the lowest lying excited state, S_1 .³⁰⁻³⁴ The more ionic $^1\text{L}_a$ state^{25,35-37} is formed predominantly by a $\text{LUMO} \leftarrow \text{HOMO}$ transition, whereas the $^1\text{L}_b$ state is primarily a combination of $\text{LUMO} \leftarrow \text{HOMO} - 1$ and $\text{LUMO} + 1 \leftarrow \text{HOMO}$.³⁸ TDDFT was used to generate the excited state configurations at B3LYP-D/6-31+G(d,p) level of theory. However, TDDFT was found to severely underestimate the $^1\text{L}_a$ energy and erroneously label it as the lowest excited state³⁹ leading to drastic errors in prediction of the emission and absorption spectra for naphthols. To circumvent this problem, all excitation energies were computed at the EOM-CCSD⁴⁰⁻⁴⁸/6-31+G(d,p) level of

theory as implemented in Q-Chem 5.0. EOM-CCSD allows us to identify the fluorescent $^1\text{L}_\text{b}$ state correctly and obtain all relative energies consistently for the various isomers of naphthols.

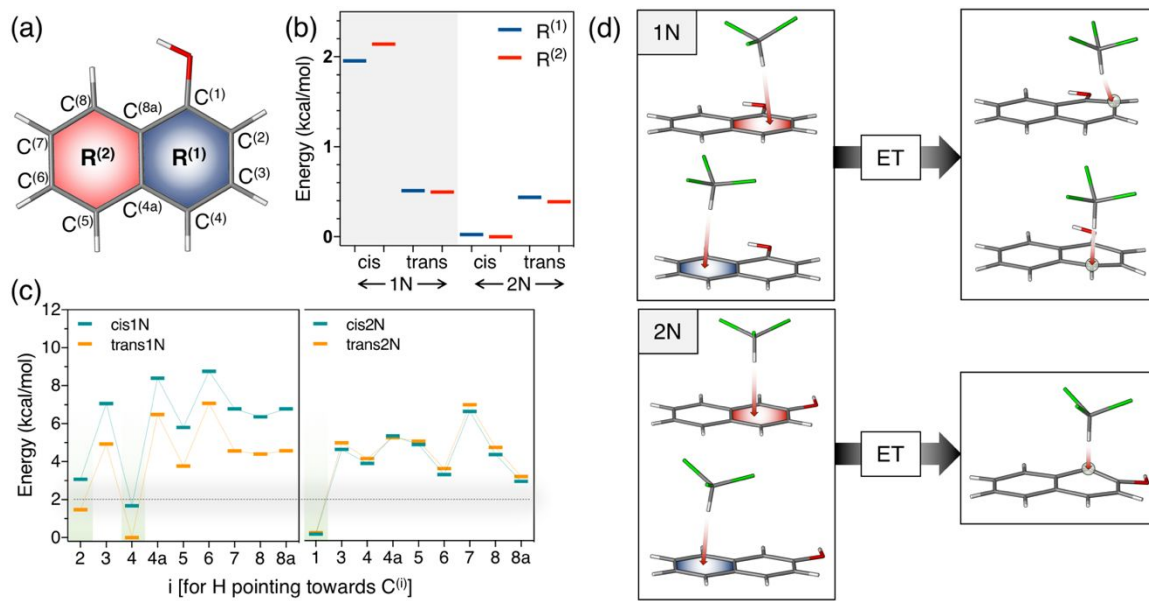


Figure 2. (a) Labelling of the aromatic rings of 1N. Energies of the 1N-CHCl₃ complex for various configurations in the (b) ground state and (c) charge-separated state. (d) Representative low energy configurations for cis1N and cis2N before and after electron transfer. Red arrows show the C-H bond pointing (left) towards the center of the ring (in the ground state) or (right) to a carbon atom (in the charge separated state).

Constrained-DFT (CDFT) optimizations provided the charge-separated (CS) state, as generated by photoinduced electron transfer, with the hole (*i.e.*, missing electron) constrained on the naphthol (donor) and the electron on the CHCl₃ (acceptor) molecule (Fig. 3). Preliminary CDFT calculations (see SI) show that CHCl₃⁻ dissociates into CHCl₂ and Cl⁻, consistent with earlier studies.^{49,50} Since the dissociation succeeds the electron transfer, it is not relevant for this study of ultrafast dynamics of photoinduced electron transfer. Therefore, we analyze the CS state with constraints on the C-Cl and C-H bond lengths derived from a separate optimization of CHCl₃⁻ at the MP2/6-311++G(d,p)

1
2
3 level of theory. This allows us to model the acceptor moiety after ET before pre-dissociation. We
4
5 find that, in the CS state, CHCl_3^- is placed above the naphthol ring with the C-H bond pointing
6
7 towards one of the carbons of the naphthol. To gain further insights into stable CS state
8
9 configurations, we performed optimizations with geometry constraints, and obtained a distribution
10
11 of configurations with the C-H bond of chloroform pointing towards each of the carbons of
12
13 naphthol. Due to negligible Boltzmann weights, the higher energy configurations were considered
14
15 statistically insignificant, and only the energetically favorable configurations were considered for
16
17 this study (Figure 2(c)). The more favored conformations, correspond to the C-H bond pointing
18
19 towards $\text{C}^{(2)}$ and $\text{C}^{(4)}$ of 1N, and $\text{C}^{(1)}$ of 2N (Figure 2(d)). Those configurations correspond to
20
21 resonance structures (see Supporting Information) stabilized by $\text{C}^{(2)}$ and $\text{C}^{(4)}$ that are the electron-
22
23 rich centers of 1N and 2N.
24
25
26
27
28
29
30
31
32
33
34
35
36
37
38
39
40
41
42
43
44
45
46
47
48
49
50
51
52
53
54
55
56
57
58
59
60

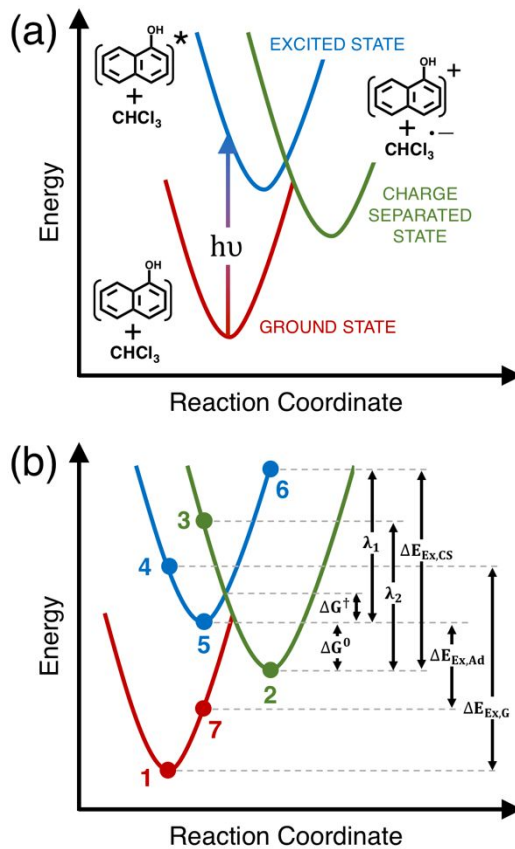


Figure 3. Schematic diagram showing the ground (red), excited (blue) and charge separated (green) energy surfaces, including formal oxidation states (a) and Marcus parameters (b) required to compute photoinduced electron transfer rates.

ET rates were computed, according to Marcus theory, using the computed parameters for the reorganization energy, electronic coupling and free energy change. Therefore, reactants and products are described by harmonic states (Figure 3(a)) at the semiclassical level.^{51–53} For weakly coupled donor-acceptor systems, the electron transfer rates (k_{ET}) depend on (i) the free energy of reaction (ΔG^0), (ii) the reorganization energy (λ), and (iii) the electronic coupling (H_{if}), as follows:

$$k_{ET} = \frac{2\pi|H_{if}|^2}{\hbar\sqrt{4\pi\lambda k_B T}} \exp\left(-\frac{(\Delta G^0 + \lambda)^2}{4\lambda k_B T}\right), \quad (1)$$

so, the ET times (t_{Comp}) can be readily obtained, as follows:

$$t_{Comp} = \frac{1}{k_{ET}}. \quad (2)$$

The free energy values (ΔG^0) are calculated as the free energy differences between the CS and excited states (Figure 3(b)):

$$\Delta G^0 = E_2 - E_5. \quad (3)$$

The reorganization energy (λ) is computed as a geometric average of the ground and CS state reorganization energies λ_1 and λ_2 (see Figure 3(b)), obtained as follows:

$$\lambda_1 = E_3 - E_2 \quad (4)$$

$$\lambda_2 = E_6 - E_5 \quad (5)$$

Under the displaced harmonic oscillator approximation,⁵⁴ $\lambda_1 = \lambda_2$. However, the two reorganization energies are usually slightly different,⁵⁵ so the effective reorganization energy (λ) is computed, as follows⁵⁵:

$$\lambda = \frac{\lambda_1 + \lambda_2}{2}. \quad (6)$$

The activation free energy (ΔG^\dagger) is defined by ΔG^0 and λ , as follows:

$$\Delta G^\dagger = \frac{(\Delta G^0 + \lambda)^2}{4\lambda}. \quad (7)$$

The electronic couplings (H_{if}) are computed with the fragment-charge difference (FCD) method,⁵⁶ under the two-state approximation (*i.e.*, assuming that the reactant and product diabatic states are linear combinations of the eigenstates). The naphthol and CHCl₃ molecules are defined as the donor and acceptor fragments, respectively. The states are chosen according to the maximum charge differences between the two fragments, as implemented in Q-Chem 5.0 at the DFT ωB97x-D/6-31+G(d,p) level of theory.

Table 1 lists the calculated Marcus parameters and ET rates. The ET from 1N is significantly faster ($t_{Comp}=16\text{--}269$ ps) than from 2N (ns), consistent with TCSPC experiments. In fact, the multiexponential fitting of the decay curves shows that the major decay time for 1N is <100 ps, while that for 2N is 1.9 ns.

Table 1. ET times and Marcus parameters

Ground State	CS State	Isomer	ΔG^0	λ	H_{if}	ΔG^\dagger	t_{Comp}	t_{TCSPC}
	H pointing to		eV					ps
$R^{(1)}$	$C^{(2)}$	cis1N	-0.41	1.35	0.01	0.16	269	
		trans1N	-0.45	1.37	0.02	0.15	85	
	$C^{(4)}$	cis1N	-0.48	1.25	0.01	0.12	51	
		trans1N	-0.51	1.27	0.02	0.11	16	70 (0.92)
$R^{(2)}$	$C^{(2)}$	cis1N	-0.42	1.34	0.02	0.16	63	1.5x10 ³ (0.08)
		trans1N	-0.45	1.34	0.02	0.15	53	
	$C^{(4)}$	cis1N	-0.48	1.37	0.02	0.15	39	
		trans1N	-0.51	1.36	0.02	0.13	29	
$R^{(1)}$		cis2N	-0.31	1.42	0.02	0.16	64	<40 (0.2)
		trans2N	-0.29	1.40	0.02	0.16	94	900 (0.4)
$R^{(2)}$	$C^{(1)}$	cis2N	-0.47	1.42	0.002	0.16	15x10 ³	1.9x10 ³ (0.4)
		trans2N	-0.46	1.39	0.001	0.16	55x10 ³	

Isomerization times <10 ps were obtained, according to transition state theory (see Table 2 and Figure 4 (a,b)) at the EOM-CCSD/6-31+G(d,p) level, using Q-Chem 5.0, with excited state barriers obtained by scanning the C^(8a)-C⁽¹⁾-O-H and C⁽¹⁾-C⁽²⁾-O-H dihedral angles.

Ultrafast isomerization leads to faster ET routes, with isomerization preceding ET. However, we observe a significantly slow component of ET and fluorescence quenching in 2N due to the noticeably slow ET in both cis- and trans-2N (with CHCl_3 pointing towards $\text{R}^{(2)}$ and nearly identical Boltzmann populations of both isomers in the excited state).

$$k_{cis \rightarrow trans} = \frac{k_B T}{\hbar} \exp\left(-\frac{\Delta E_1^*}{k_B T}\right) \quad (8)$$

$$k_{trans \rightarrow cis} = \frac{k_B T}{\hbar} \exp\left(-\frac{\Delta E_2^*}{k_B T}\right) \quad (9)$$

$$\frac{N_{cis}}{N_{trans}} = \frac{k_B T}{\hbar} \exp\left(-\frac{\Delta E_3^*}{k_B T}\right) \quad (10)$$

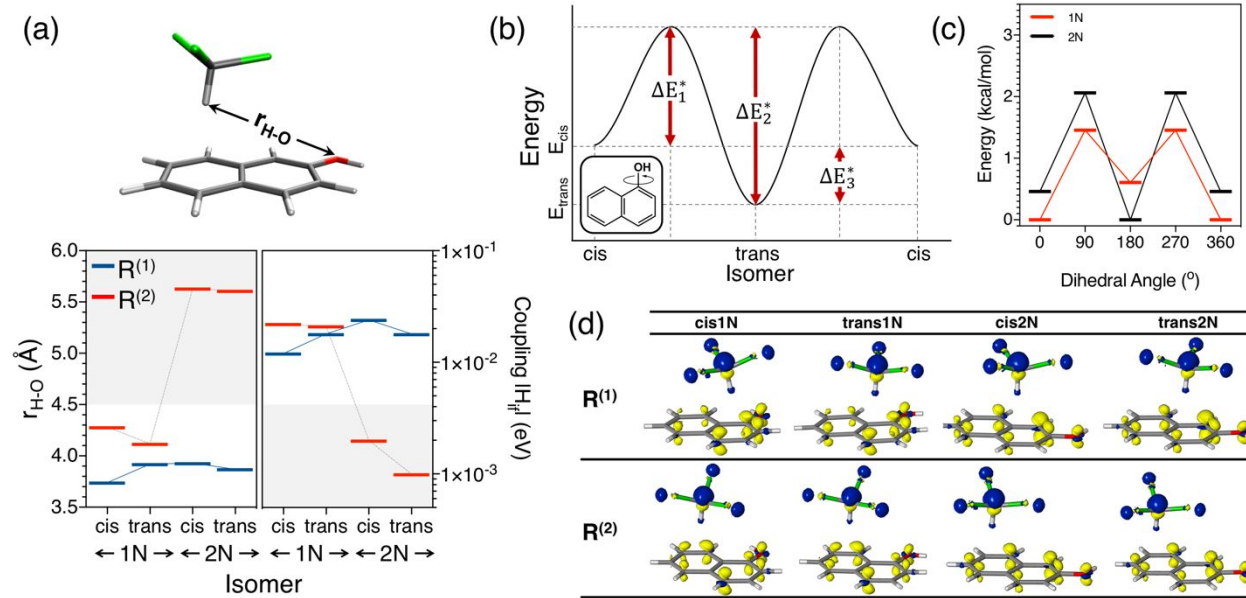


Figure 4. (a) Distances between H of CHCl_3 and O of naphthol for different configuration with the solvent on top of $\text{R}^{(1)}$ and $\text{R}^{(2)}$ and corresponding electronic couplings. (b) Schematic diagram of a dihedral scan and relevant energies. (c) Dihedral scans of $\text{C}^{(8a)}-\text{C}^{(1)}-\text{O}-\text{H}$ (for 1N) and $\text{C}^{(1)}-\text{C}^{(2)}-\text{O}-\text{H}$ (for 2N) in the excited state. (d) Change of electron density before and after electron transfer (density goes from yellow to blue during ET).

Table 2. Excited state isomerization times and Boltzmann populations.

Molecule	Isomer	Isomerization Time ps	Population %
1N	cis	3	76
	trans	1	24
2N	cis	4	52
	trans	8	48

As noted from Table 1, configurations with low ΔG^0 also have low λ , resulting in similar ΔG^\dagger for all the cases. Electronic couplings are thus important factors that modulate ET rates.

The plot of electron densities differences, before and after ET (Figure 4(d)), shows that the electron density is transferred from the oxygen of the naphthol to the CHCl_3 molecule. Being on top of $\text{R}^{(1)}$ allows the solvent molecule to accept the electron much faster. However, when the electron accepting solvent molecule is on top of $\text{R}^{(2)}$, especially for 2N, ET is slower since the separation between the electron rich oxygen and the CHCl_3 is larger and thus the electronic coupling is significantly smaller (Figure 4(c)).

In summary, quantum chemical calculations on several statistically relevant configurations allowed us to elucidate the origin of significantly different fluorescence lifetimes of photoexcited naphthols in halogenated solvents. The observed differences in ET dynamics stem from the differences in electronic couplings, when comparing 1N and 2N. Differences in reorganization energies are nearly compensated by concomitant differences in ET free energy changes. The differences in couplings are controlled by different electron donor-acceptor distances, as determined by the closer contact of the $-\text{OH}$ group with CHCl_3 in 1N when compare to 2N, thereby rationalizing the significantly different fluorescence quenching lifetimes observed in experiments.

1
2
3 Our findings suggest that increasing the number of fused aromatic rings in the chromophore can
4 allow us to gain control over fluorescence quenching times through modulation of the separation
5 between the electron accepting solvent molecules in the first coordination sphere and the electron
6 rich center of the -OH substituted acenes. The regioselective ET discussed in this study can be
7 utilized for several practical applications, an evident one being the design of photo-switching
8 molecular probes.
9
10
11
12
13
14
15
16
17

ASSOCIATED CONTENT

Supporting Information

24 The Supporting Information is available free of charge on the ACS Publications website at DOI:
25
26 XXXXXXXXX.
27
28

29 Computational method, information about calculations performed, necessity of using EOM-CCSD
30 for excited states, comparison of free and reorganization energies with and without explicit solvent,
31 coordinates of optimized structures
32
33
34
35
36

AUTHOR INFORMATION

Corresponding Author

43 *E-mail: victor.batista@yale.edu
44
45
46

47 The authors declare no competing financial interest.
48
49

ACKNOWLEDGEMENTS

53 V.S.B. acknowledges support by the AFOSR grant #FA9550-17- 0198 and high-performance
54 computing time from NERSC. This work used the Extreme Science and Engineering Discovery
55
56
57
58

1
2
3 Environment (XSEDE), which is supported by National Science Foundation grant number ACI-
4 1053575. A.A. acknowledges supercomputer time from the Extreme Science and Engineering
5 Discovery Environment (XSEDE) under Grant TG-CHE170024. E.T.J.N. acknowledges support
6 from the German Science Foundation (Project Nr. DFG - NI 492/11-1).
7
8
9
10
11
12

13 REFERENCES

14

15
16 (1) Grätzel, M. Solar Energy Conversion by Dye-Sensitized Photovoltaic Cells. *Inorg. Chem.*
17 **2005**, *44* (20), 6841–6851.
18 (2) Gust, D.; Moore, T. A.; Moore, A. L. Solar Fuels via Artificial Photosynthesis. *Acc. Chem.*
19 *Res.* **2009**, *42* (12), 1890–1898.
20 (3) Polívka, T.; Sundström, V. Ultrafast Dynamics of Carotenoid Excited States—From Solution
21 to Natural and Artificial Systems. *Chem. Rev.* **2004**, *104* (4), 2021–2072.
22 (4) Bottari, G.; de la Torre, G.; Guldi, D. M.; Torres, T. Covalent and Noncovalent
23 Phthalocyanine–Carbon Nanostructure Systems: Synthesis, Photoinduced Electron Transfer,
24 and Application to Molecular Photovoltaics. *Chem. Rev.* **2010**, *110* (11), 6768–6816.
25 (5) Nelson, N.; Yocom, C. F. STRUCTURE AND FUNCTION OF PHOTOSYSTEMS I AND
26 II. *Annu. Rev. Plant Biol.* **2006**, *57* (1), 521–565.
27 (6) Bixon, M.; Jortner, J. Electron Transfer—from Isolated Molecules to Biomolecules. *Adv.*
28 *Chem. Phys. Electron Transfer—from Isol. Mol. Biomol. Part 1* **1999**, *106*, 35–202.
29 (7) Pellegrin, Y.; Odobel, F. Molecular Devices Featuring Sequential Photoinduced Charge
30 Separations for the Storage of Multiple Redox Equivalents. *Coord. Chem. Rev.* **2011**, *255*
31 (21–22), 2578–2593.
32 (8) Gilat, S. L.; Kawai, S. H.; Lehn, J.-M. Light-Triggered Molecular Devices: Photochemical
33 Switching of Optical and Electrochemical Properties in Molecular Wire Type Diarylethene
34 Species. *Chem. - Eur. J.* **1995**, *1* (5), 275–284.
35 (9) Holten, D.; Bocian, D. F.; Lindsey, J. S. Probing Electronic Communication in Covalently
36 Linked Multiporphyrin Arrays. A Guide to the Rational Design of Molecular Photonic
37 Devices. *Acc. Chem. Res.* **2002**, *35* (1), 57–69.
38 (10) Meier, H. Conjugated Oligomers with Terminal Donor–Acceptor Substitution. *Angew.*
39 *Chem. Int. Ed.* **2005**, *44* (17), 2482–2506.
40 (11) Kumpulainen, T.; Lang, B.; Rosspeintner, A.; Vauthey, E. Ultrafast Elementary
41 Photochemical Processes of Organic Molecules in Liquid Solution. *Chem. Rev.* **2017**, *117*
42 (16), 10826–10939.
43 (12) Koch, M.; Rosspeintner, A.; Adamczyk, K.; Lang, B.; Dreyer, J.; Nibbering, E. T. J.;
44 Vauthey, E. Real-Time Observation of the Formation of Excited Radical Ions in Bimolecular
45 Photoinduced Charge Separation: Absence of the Marcus Inverted Region Explained. *J. Am.*
46 *Chem. Soc.* **2013**, *135* (26), 9843–9848.
47 (13) Dance, Z. E. X.; Ahrens, M. J.; Vega, A. M.; Ricks, A. B.; McCamant, D. W.; Ratner, M. A.;
48 Wasielewski, M. R. Direct Observation of the Preference of Hole Transfer over Electron
49 Transfer for Radical Ion Pair Recombination in Donor–Bridge–Acceptor Molecules. *J. Am.*
50 *Chem. Soc.* **2008**, *130* (3), 830–832.
51
52
53
54
55
56
57
58
59
60

(14) Closs, G. L.; Miller, J. R. Intramolecular Long-Distance Electron Transfer in Organic Molecules. *Science* **1988**, *240* (4851), 440–447.

(15) Miller, J. R.; Calcaterra, L. T.; Closs, G. L. Intramolecular Long-Distance Electron Transfer in Radical Anions. The Effects of Free Energy and Solvent on the Reaction Rates. *J. Am. Chem. Soc.* **1984**, *106* (10), 3047–3049.

(16) Shirota, H.; Pal, H.; Tominaga, K.; Yoshihara, K. Substituent Effect and Deuterium Isotope Effect of Ultrafast Intermolecular Electron Transfer: Coumarin in Electron-Donating Solvent. *J. Phys. Chem. A* **1998**, *102* (18), 3089–3102.

(17) Ghosh, H. N.; Verma, S.; Nibbering, E. T. J. Ultrafast Forward and Backward Electron Transfer Dynamics of Coumarin 337 in Hydrogen-Bonded Anilines As Studied with Femtosecond UV-Pump/IR-Probe Spectroscopy. *J. Phys. Chem. A* **2011**, *115* (5), 664–670.

(18) Castner, E. W.; Kennedy, D.; Cave, R. J. Solvent as Electron Donor: Donor/Acceptor Electronic Coupling Is a Dynamical Variable. *J. Phys. Chem. A* **2000**, *104* (13), 2869–2885.

(19) Scherer, P. O. J.; Tachiya, M. Computer Simulation Studies of Electron Transfer Parameters for Cyanoanthracene/N,N-Dimethylaniline Solutions. *J. Chem. Phys.* **2003**, *118* (9), 4149–4156.

(20) Morandeira, A.; Fürstenberg, A.; Gumi, J.-C.; Vauthey, E. Fluorescence Quenching in Electron-Donating Solvents. 1. Influence of the Solute–Solvent Interactions on the Dynamics. *J. Phys. Chem. A* **2003**, *107* (28), 5375–5383.

(21) Morandeira, A.; Fürstenberg, A.; Vauthey, E. Fluorescence Quenching in Electron-Donating Solvents. 2. Solvent Dependence and Product Dynamics. *J. Phys. Chem. A* **2004**, *108* (40), 8190–8200.

(22) Saik, V. O.; Goun, A. A.; Fayer, M. D. Photoinduced Electron Transfer and Geminate Recombination for Photoexcited Acceptors in a Pure Donor Solvent. *J. Chem. Phys.* **2004**, *120* (20), 9601–9611.

(23) Rosspeintner, A.; Angulo, G.; Vauthey, E. Driving Force Dependence of Charge Recombination in Reactive and Nonreactive Solvents. *J. Phys. Chem. A* **2012**, *116* (38), 9473–9483.

(24) Chaudhuri, S.; Rudshteyn, B.; Prémont-Schwarz, M.; Pines, D.; Pines, E.; Huppert, D.; Nibbering, E. T.; Batista, V. S. Ultrafast Photo-Induced Charge Transfer of 1-Naphthol and 2-Naphthol to Halocarbon Solvents. *Chem. Phys. Lett.* **2017**, *683*, 49–56.

(25) Messina, F.; Prémont-Schwarz, M.; Braem, O.; Xiao, D.; Batista, V. S.; Nibbering, E. T. J.; Chergui, M. Ultrafast Solvent-Assisted Electronic Level Crossing in 1-Naphthol. *Angew. Chem. Int. Ed.* **2013**, *52* (27), 6871–6875.

(26) Cossi, M.; Rega, N.; Scalmani, G.; Barone, V. Energies, Structures, and Electronic Properties of Molecules in Solution with the C-PCM Solvation Model. *J. Comput. Chem.* **2003**, *24* (6), 669–681.

(27) Shao, Y.; Gan, Z.; Epifanovsky, E.; Gilbert, A. T.; Wormit, M.; Kussmann, J.; Lange, A. W.; Behn, A.; Deng, J.; Feng, X.; et al. Advances in Molecular Quantum Chemistry Contained in the Q-Chem 4 Program Package. *Mol. Phys.* **2015**, *113* (2), 184–215.

(28) Becke, A. D. Density-functional Thermochemistry. III. The Role of Exact Exchange. *J. Chem. Phys.* **1993**, *98* (7), 5648–5652.

(29) Chai, J.-D.; Head-Gordon, M. Long-Range Corrected Hybrid Density Functionals with Damped Atom–Atom Dispersion Corrections. *Phys. Chem. Chem. Phys.* **2008**, *10* (44), 6615–6620.

1
2
3
4
5
6
7
8
9
10
11
12
13
14
15
16
17
18
19
20
21
22
23
24
25
26
27
28
29
30
31
32
33
34
35
36
37
38
39
40
41
42
43
44
45
46
47
48
49
50
51
52
53
54
55
56
57
58
59
60

(30) Suzuki, S.; Baba, H. Polarization Study of the Fluorescent State of the Hydrogen Bonded α -Naphthol. *Bull. Chem. Soc. Jpn.* **1967**, *40* (9), 2199–2200.

(31) Magnes, B.-Z.; Strashnikova, N. V.; Pines, E. Evidence for 1La, 1Lb Dual State Emission in 1-Naphthol and 1-Methoxynaphthalene Fluorescence in Liquid Solutions. *Isr. J. Chem.* **1999**, *39* (3–4), 361–373.

(32) Knochenmuss, R.; Muñoz, P. L.; Wickleder, C. Vibronic Coupling and Microscopic Solvation of 1-Naphthol. *J. Phys. Chem.* **1996**, *100* (27), 11218–11227.

(33) Suzuki, S.; Fujii, T.; Imai, A.; Akahori, H. The Fluorescent Level Inversion of Dual Fluorescences and the Motional Relaxation of Excited State Molecules in Solutions. *J. Phys. Chem.* **1977**, *81* (16), 1592–1598.

(34) Suzuki, S.; Fujii, T.; Sato, K. The Temperature Dependence of the Fluorescence and Polarization Spectra of 1-Naphthol. *Bull. Chem. Soc. Jpn.* **1972**, *45* (6), 1937–1938.

(35) Grimme, S.; Parac, M. Substantial Errors from Time-Dependent Density Functional Theory for the Calculation of Excited States of Large π Systems. *ChemPhysChem* **2003**, *4* (3), 292–295.

(36) Richard, R. M.; Herbert, J. M. Time-Dependent Density-Functional Description of the 11a State in Polycyclic Aromatic Hydrocarbons: Charge-Transfer Character in Disguise? *J. Chem. Theory Comput.* **2011**, *7* (5), 1296–1306.

(37) Wong, B. M.; Hsieh, T. H. Optoelectronic and Excitonic Properties of Oligoacenes: Substantial Improvements from Range-Separated Time-Dependent Density Functional Theory. *J. Chem. Theory Comput.* **2010**, *6* (12), 3704–3712.

(38) Xiao, D.; Prémont-Schwarz, M.; Nibbering, E. T. J.; Batista, V. S. Ultrafast Vibrational Frequency Shifts Induced by Electronic Excitations: Naphthols in Low Dielectric Media. *J. Phys. Chem. A* **2012**, *116* (11), 2775–2790.

(39) Acharya, A.; Chaudhuri, S.; Batista, V. S. Can TDDFT Describe Excited Electronic States of Naphthol Photoacids? A Closer Look with EOM-CCSD. *J. Chem. Theory Comput.* **2018**, *14* (2), 867–876.

(40) Rowe, D. Equations-of-Motion Method and the Extended Shell Model. *Rev. Mod. Phys.* **1968**, *40* (1), 153.

(41) Emrich, K. An Extension of the Coupled Cluster Formalism to Excited States:(II). Approximations and Tests. *Nucl. Phys. A* **1981**, *351* (3), 397–438.

(42) Geertsen, J.; Rittby, M.; Bartlett, R. J. The Equation-of-Motion Coupled-Cluster Method: Excitation Energies of Be and CO. *Chem. Phys. Lett.* **1989**, *164* (1), 57–62.

(43) Stanton, J. F.; Bartlett, R. J. The Equation of Motion Coupled-Cluster Method. A Systematic Biorthogonal Approach to Molecular Excitation Energies, Transition Probabilities, and Excited State Properties. *J. Chem. Phys.* **1993**, *98* (9), 7029–7039.

(44) Krylov, A. I. Equation-of-Motion Coupled-Cluster Methods for Open-Shell and Electronically Excited Species: The Hitchhiker’s Guide to Fock Space. *Annu Rev Phys Chem* **2008**, *59*, 433–462.

(45) Stanton, J. F.; Gauss, J. A Discussion of Some Problems Associated with the Quantum Mechanical Treatment of Open-Shell Molecules. *Adv. Chem. Phys.* **2003**, *125*, 101–146.

(46) Comeau, D. C.; Bartlett, R. J. The Equation-of-Motion Coupled-Cluster Method. Applications to Open-and Closed-Shell Reference States. *Chem. Phys. Lett.* **1993**, *207* (4–6), 414–423.

(47) Stolarszky, L. Z.; Monkhorst, H. J. Coupled-Cluster Method with Optimized Reference State. *Int. J. Quantum Chem.* **1984**, *26* (S18), 267–291.

1
2
3 (48) Sinha, D.; Mukhopadhyay, S.; Mukherjee, D. A Note on the Direct Calculation of Excitation
4 Energies by Quasi-Degenerate MBPT and Coupled-Cluster Theory. *Chem. Phys. Lett.* **1986**,
5 129 (4), 369–374.
6 (43) Staneke, P. O.; Groothuis, G.; Ingemann, S.; Nibbering, N. M. M. Formation, Stability and
7 Structure of Radical Anions of Chloroform, Tetrachloromethane and Fluorotrichloromethane
8 in the Gas Phase. *Int. J. Mass Spectrom. Ion Process.* **1995**, 142 (1–2), 83–93.
9 (50) Isse, A. A.; Lin, C. Y.; Coote, M. L.; Gennaro, A. Estimation of Standard Reduction
10 Potentials of Halogen Atoms and Alkyl Halides. *J. Phys. Chem. B* **2010**, 115 (4), 678–684.
11 (45) Marcus, R. A. Electron Transfer Reactions in Chemistry. Theory and Experiment. *Rev. Mod.*
12 *Phys.* **1993**, 65 (3), 599–610.
13 (46) Marcus, R. A. On the Theory of Oxidation-Reduction Reactions Involving Electron Transfer.
14 *I. J. Chem. Phys.* **1956**, 24 (5), 966–978.
15 (53) Chaudhuri, S.; Hedström, S.; Méndez-Hernández, D. D.; Hendrickson, H. P.; Jung, K. A.;
16 Ho, J.; Batista, V. S. Electron Transfer Assisted by Vibronic Coupling from Multiple Modes.
17 *J. Chem. Theory Comput.* **2017**, 13 (12), 6000–6009.
18 (48) Marcus, R. A.; Sutin, N. Electron Transfers in Chemistry and Biology. *Biochim. Biophys.*
19 *Acta BBA - Rev. Bioenerg.* **1985**, 811 (3), 265–322.
20 (55) Parson, W. W.; Chu, Z. T.; Warshel, A. Reorganization Energy of the Initial Electron-
21 Transfer Step in Photosynthetic Bacterial Reaction Centers. *Biophys. J.* **1998**, 74 (1), 182–
22 191.
23 (56) Voityuk, A. A.; Rösch, N. Fragment Charge Difference Method for Estimating Donor–
24 Acceptor Electronic Coupling: Application to DNA π -Stacks. *J. Chem. Phys.* **2002**, 117 (12),
25 5607–5616.
26
27
28
29
30
31
32
33
34
35
36
37
38
39
40
41
42
43
44
45
46
47
48
49
50
51
52
53
54
55
56
57
58
59
60